Chapter 9

Pyrolysis of Paper Mill Waste: Effect of Montmorillonite Clay

Abstract

The thermal degradation of paper mill waste (PMW) has been investigated in presence and absence of Montmorillonite clay in the temperature range of ambient to 1000^{o}C and at the heating rates of 20, 25and 30^{o}C/min. Proximate and ultimate analyses and evaluation of calorific value (HHV) of PMW has been carried out using standard protocols. The thermo-gravimetric analysis (TGA) and differential thermogravimetric (DTG) data obtained under both situations have been used to evaluate the kinetic and thermodynamic parameters and elucidate the reaction mechanism. The clay has also been characterized using TGA/DTG analysis, Fourier Transform Infra-Red (FTIR) spectroscopic analysis and X-ray diffraction (XRD), Energy dispersive spectroscopy (EDS), and scanning electron microscopic (SEM) techniques. The activation energy, pre-exponential factor and thermodynamic parameters have been evaluated using the model-free iso-conversional method of Flynn-Wall-Ozawa (FWO) and Vyazovkin and the distributed activation energy model (DAEM). The Montmorillonite clay has influenced the degradation process appreciably through its catalytic action.

9.1 Introduction

Pulp and paper mills are one of the important industrial units that contribute towards the financial advancement and overall development of a nation (Raut et al., 2012). In India also these mills play a crucial role in the overall development. Most pulp and paper mills meet greater part of their energy requirements from the solid waste biomass from processes (“Annual Report 2017‑18,” 2017). On the basis of the feedstock being used the pulp and paper mills are put mainly under three categories namely wood-based, agro waste-based and recycled fibre-based. From these mills different types of energy-rich biomass wastes

produces. According to the Central Pulp and Paper Research Institute, India, the useful portion of the feedstock used in paper mills depends upon its nature. For agro-waste (bagasse and wheat straw)based mills it is only 10%, for wood based mills it is 26% and for wastepaper based mills it is 64% and the rest is treated as the waste biomass("Annual Report 2017-18," 2017). These wastes are produced from different stages of paper making for example, black liquor from Kraft mills bark and wood residues from mechanical pulping and rejects from cleaning and screening operations (Annual Report 2017-18," 2017). In several mills such wastes are burnt internally for generating energy in conventional way, but the process used is not very efficient. There is need to improve the conventional methods. For converting paper mills waste through pyrolysis to bio-oil, gas and char it is important to know the kinetics of thermal decomposition process and the nature of waste decomposition products (Sriram and Swaminathan, 2018). The inevitable target of the pyrolysis is to yield high-value energy products for replacing and/or supplementing fast depleting non-renewable petroleum products (Huang et al., 2011; Kumar et al., 2019b; Mishra and Bhaskar, 2014)

9.2 Collection of paper mill waste

The paper mill waste (PMW) was collected from M/s Yash Paper Limited, Faizabad, India, a sugar-cane bagasse based paper mill. The PMW comprise the rejects from the cleaning and screening processes of the sugar cane bagasse produced during the mechanical pulping. The PMW sample collected from the mill was air-dried for two days and then in a hot air oven (103 ± 2 °C) for 4–6 h before grinding. The dried PMW sample was pulverized in a grinding mill (Model 2, Arthur H. Thomas. Co, Philadelphia, USA) and sieved to collect

the particles of 60–80 mesh size (0.180–0.250 mm). The screened PMW powder was packed in an airtight plastic container for further analysis and pyrolysis experiments. The Montmorillonite clay was obtained from Sigma Aldrich (99.0%, Sigma Aldrich, USA) and was used in all experiments after calcination at 600 °C for 4 h with a heating rate of 5 °C/min.

9.3 Thermochemical characteristics of PMW

The ASTM protocol (ASTM E870-82) was followed for estimating volatile matter (VM), ash content (AC) and fixed carbon (FC) content of the PMW powder. The moisture content (MC) was determined using a moisture analyzer (Wensar, An ISO 9001. India). The fixed carbon (FC) was calculated by difference using equation: Fixed carbon (%) = 100 − {MC (%) + VM (%) + Ash content (%)}. The CHNS analyzer (Euro EA 3000, Elemental Analyzer, Italy) was used for estimating the carbon, hydrogen, nitrogen, and sulfur contents. The oxygen content was determined by the difference. The higher heating value (HHV, MJ/kg) of the sample was determined using a bomb calorimeter (Model- RSB 3, Rajdhani Scientific Inst. Co. New Delhi, India). The detection of the functional groups of the chemical compounds in the powdered PMW sample was carried out using a Fourier Transform Infra-red (FTIR) spectroscope (NICOLET 5700 FTIR, Thermo-electron Corporation, USA) in the wave number range of 400–4000cm^{-1}.

9.4 Characterization of Montmorillonite clay catalyst

The crystalline structure of the clay was ascertained through X-ray diffraction (XRD) analysis using a Rigaku X-RD unit (Smart Lab, 9 kW Powder Type (without χcradle, Japan). The FTIR spectroscopic analysis was used to ascertain the functional groups

present in the clay. The scanning electron microscope (EVO - Scanning Electron Microscope MA15/18, Carl Zeiss Microscopy Ltd, Germany) was used to know the surface morphology of clay particles. The SEM unit was also connected with an energy-dispersive X-ray spectroscopic (EDS) unit (51N1000- EDS System, Oxford Instruments NanoAnalysis; United Kingdom). The thermal stability of the clay was studied using the TGA/DTG unit (Model 00377, TGA-50, Shimadzu Corp. Japan) in nitrogen atmosphere (flow rate = 100 ml/min) in the temperature range of ambient to 1000°C. Approximately 6–8 mg accurately weighed sample was taken for TGA experiment. To reduce the heat transfer resistance between the thermocouples and the crucible, a platinum crucible was used.

9.5 Thermogravimetric analysis (TGA)

The thermal degradation of the dried PMW and its mixture with clay catalyst (in equal ratio) was studied using the TGA/DTG unit mentioned above at three different heating rates of 20, 25 and 30°C/min in the temperature range of ambient to 1000°C. Approximately 6–8mg accurately weighed well mixed sample was taken for each experiment. The variation of %weight loss versus time (s) or temperature (°C) was recorded at each heating rate for PMW and clay-PMW mixture samples. All the experiments were repeated at least two times to check the reproducibility of data and mean values were used for further analysis of results. The differential thermo-gravimetric (DTG) data were also generated for each sample at each heating rate by differentiating the data with respect to time using the Origin pro-software.

9.6 Results and discussion

9.6.1 Thermochemical characteristics

The Thermochemical properties (moisture, ash, fixed carbon and volatile matter contents; carbon, hydrogen, nitrogen, sulphur, and oxygen contents, and higher heating values) of PMW are presented in Table 9.1along with the reported values for sugar cane bagasse (Jayaraman et al., 2018) and wheat straw (Kumar et al., 2019c). It can be seen from Table 9.1 that the moisture and ash contents of PMW are less than those of bagasse and wheat straw indicating its superiority as feedstock for thermal conversion. The moisture requires energy to evaporate and ash (primarily inorganic fraction) does not contribute to the HHV rather it will consume some energy for oxidation to oxides(García et al., 2012; Motghare et al., 2016). The volatile matter and fixed carbon indicate ease of ignition and combustion. Both VM and FC have carboxylic acid, hydrocarbon, phenols and tars as their constituents (Vassilev et al., 2010).The volatile matter and fixed carbon contents of PMW are comparable to published values for sugar cane bagasse and wheat straw(Table 9.1). High values of carbon (53.75%) and hydrogen (4.57%) contents indicate suitability of PMW for conversion in to valuable gaseous and liquid fuels through pyrolysis or gasification process. It is interesting to note that the PMW has very low nitrogen content (1.01%) and no sulphur. Therefore, its combustion will not result in emission of any SO_x. Further, due to its low combustion temperature and low inherent nitrogen content, the formation of fuel and thermal NO_x will also be low. The HHV of PMW, estimated to be 19 MJ/kg is high making it suitable as a fuel (Kumar et al., 2019c).

The Fourier transform infrared (FTIR) spectra of paper mill waste (PMW) were recorded to identify the functional groups in the wavenumber range of 500cm^{-1} to 4000cm^{-1} (Fig. 9.2). The peak around 3200$cm^{-1}$is due to the –OH group stretching of alcohols and phenols

(Kumar et al., 2019a). Peaks between 3100cm^{-1} and 2840cm^{-1} are attributed to the C-H stretching of alkane and alkene. A weak peak at 2220cm^{-1} is due to the C≡C stretching of alkyne. Another weak peak observed at 1857cm^{-1} is due the C=O stretching of anhydride. The peak at 1549cm^{-1} corresponds to the N-H group of nitro compounds. The peaks of medium intensity observed from 1409 to 1218cm^{-1}, are due the O-H bending of alcohol and carboxylic acid.

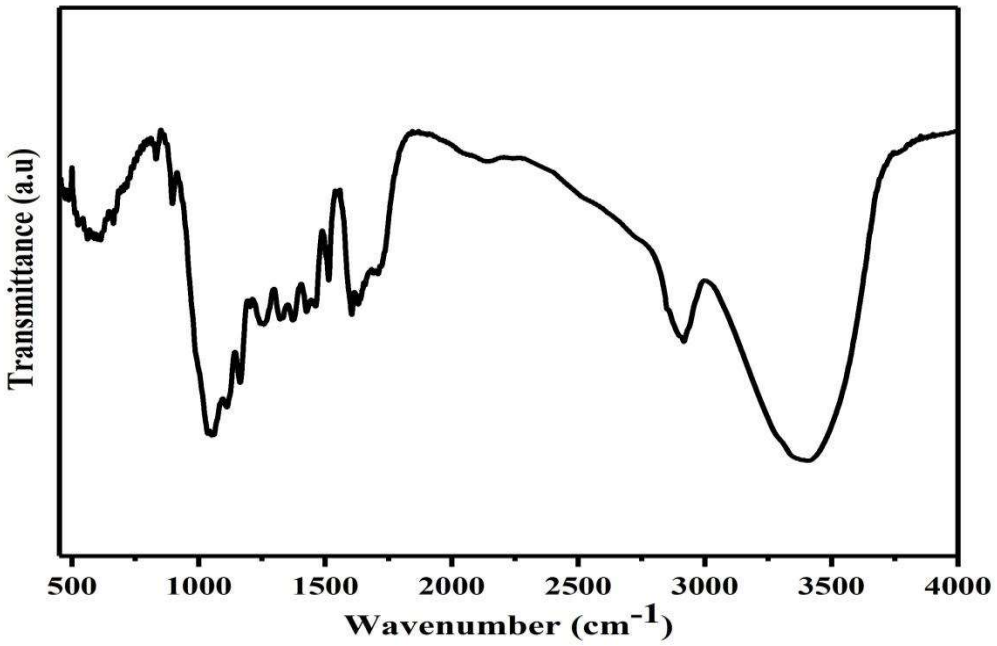

Fig 9.1: FTIR spectra of paper mill waste (PMW)

Table 9.1: Physicochemical properties of paper mill waste with published work

Sample	Moisture content (%)	Ash content (%)	Volatile matter (%)	Fixed carbon (%)	Higher heating values (MJ/kg)	Carbon (%)	Hydrogen (%)	Nitrogen (%)	Sulphur (%)	Oxygen (%)
PMW (This work)	5.86	6.50	77.90	9.74	19.00	53.75	4.57	1.01	-	40.67
Wheat straw	7.67	7.00	78.33	7.00	15.29	48.24	5.64	0.56	-	45.55
Sugar cane bagasse	8.30	9.10	72.00	10.60	-	44.26	5.76	-	-	40.88

Table 9.2: TGA and DTG analysis of paper mill waste

	PMW						PMW+Clay					
Heating rate (^oC/min)	T_i	T_f	T_p	DTG_p (%/min)	Weight loss (%)	Residual weight (%)	T_i	T_f	T_p	DTG_p (%/min)	Weight loss (%)	Residual weight (%)
Stage I												
20	28.52	232.89	71.00	0.08	8.37		28.56	232.89	54.80	0.65	15.00	
25	28.62	240.00	86.00	0.07	9.68		30.95	240.00	90.26	0.63	16.82	
30	35.34	250.00	64.00	0.04	8.05		34.24	250.00	75.86	0.69	11.13	
Stage II												
20	232.00	440.00	341.00	0.64	68.25		232.00	440.00	350.00	2.58	56.00	
25	240.00	445.00	354.00	0.54	65.29		240.00	445.00	393.00	3.08	55.89	
30	250.00	450.00	387.00	0.45	59.96		250.00	450.00	397.00	3.53	55.69	
Stage III												
20	440.00	1000.0	440.00	0.23	16.52	6.86	440.00	1000.0	440.00	0.82	22.72	6.30
25	445.00	1000.0	445.00	0.19	18.86	6.17	445.00	1000.0	445.00	0.41	19.40	6.03
30	450.00	1000.0	450.00	0.05	10.14	20.80	450.00	1000.0	450.00	0.34	14.90	17.28

9.6.2 Characterization of Montmorillonite Clay

The FTIR spectra of Montmorillonite clay were recorded in the wavenumber range of 500 to 4000cm^{-1} (Fig 9.2 (a)). The peak at around 500cm^{-1} denotes the presence of small quantity of C-I and C-F groups. The peak corresponding to 800 and 1100cm^{-1} is due to the asymmetric stretching vibrations of the Si-O-Si and because of the AlO_4 and SiO_4 groups of Montmorillonite clay (Balasundram et al., 2018; Zakaria et al., 2012). The peak at 1600cm^{-1} is due to the water molecule present in the clay. The peaks in the range of 3430–3700 cm^{-1} are attributed to the Si-OH group of extra-framework aluminum species (AlOHefs) (Balasundram et al., 2018; Cheng and Huber, 2011). The X-Ray diffraction pattern has been obtained in the 2θ range of 10-90^o to know the crystallinity and purity (Fig 9.2 (b)). The main XRD peaks of Montmorillonite clay are observed at 2θ of 18.06°, 19.98°, 21.12°, and 26.94°, thus it can be inferred that there is no extra peak is observed for the metal oxide. The scanning electron microscopic (SEM) analysis of clay was also carried out (Fig 9.2 (c)). The agglomeration of particles has been observed due to the presence of metals in clay and this may be possibly due the interconnection of metals (Balasundram et al., 2018). The EDS analysis of clay confirmed the presence of metals (Fig. 9.2(d)). The silicon (Si) content was found to be higher than aluminum (Al), sodium (Na), magnesium (Mg), calcium (Ca) contents. Similar nature of Montmorillonite clay was also reported by Singla et al. (2012).

The thermal stability of the clay was studied using thermo-gravimetric analyzer (TGA/DTG) (Fig 9.2 (e)-(f)). Maximum weight loss (~ 4.5 %) was observed up to 150^{o}C at the rate of 1.9%/min. This weight loss is due to the removal of the moisture from the clay. Between 150 to 1000^{o}C, there is negligible weight loss. Thus it can be inferred that the clay

undergoes practically no significant degradation in the temperature range used for the pyrolysis of PMW.

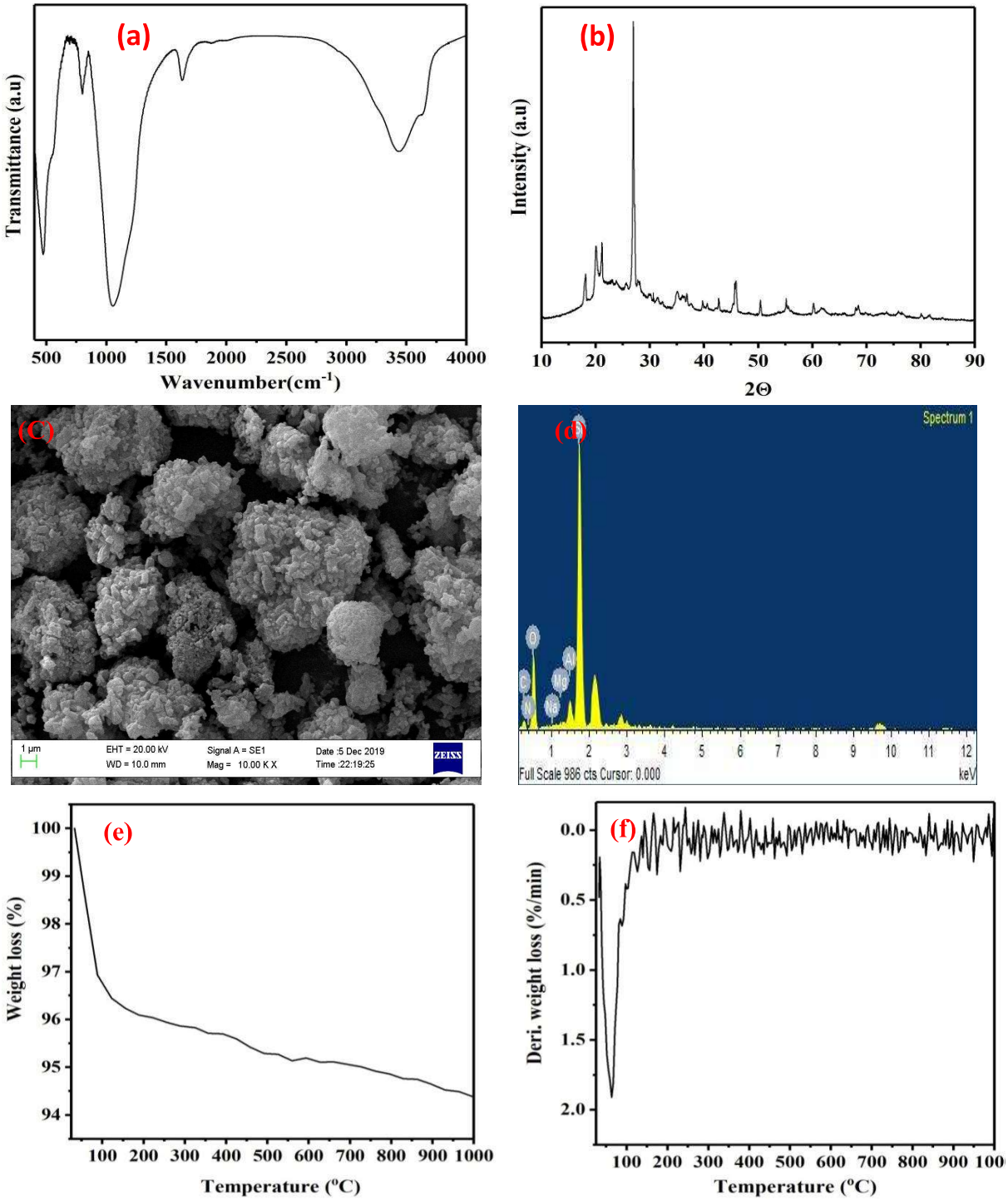

Fig. 9.2: Characterization of MMT clay: (a) FTIR spectra, (b) XRD pattern (c) SEM image (d) EDS analysis (e) TGA analysis (f) DTG analysis

9.6.3 Thermogravimetric analysis (TGA)

The thermal degradation behaviour of paper mill waste (PMW) has been investigated using a TGA/DTA unit between ambient (30^{o}C) to 1000^{o}C in the presence of nitrogen. The TGA and DTG curves for the heating rate of 30^{o}C/min are shown in Fig. 9.3 (a) as a typical example. It is seen that the TGA/DTG curve can be divided in three broad stages: Stage 1 (30 to 250^{o}C) during which the removal of moisture and lighter fractions of volatile matter occurs, Stage 2 (250 to 450^{o}C) where the thermal degradation of hemicellulose and cellulose contents of PMW and other volatile molecules takes place, and Stage 3 (above 450^{o}C, up to 1000^{o}C) during which majorly the decomposition of lignin takes place. In Stage 1 about7% weight loss has been observed and is nearly equal to the moisture content (5.86%) as estimated through the proximate analysis. In Stage 2 the total weight loss is found to be 61% and is due to the thermal degradation of hemicellulose and celluloses. The high weight loss region observed in this stage is attributed to the breaking of bonds and formation of smaller gaseous and liquid molecules (Kumar et al., 2020). Some of the degradation products recombine to give new products that are responsible for higher yield of bio-oil. Thus, this stage is also termed as the active pyrolysis stage. The total weight loss in Stage 3 is found to be 10.14%. This lowering of weight loss can be attributed to the formation of char. It is the highest temperature range stage among the three stages. Therefore at higher temperature, the formation of CO and CO_2 may be taking place due to the oxidation of non-volatile carbon molecules(Mishra and Mohanty, 2018)

The differential thermogravimetric (DTG) analyses results for both catalytic and non-catalytic pyrolysis of PMW are also shown in Fig. 9.3(a). The DTG analysis helps in determining the rate of decomposition with increase in temperature in different stages of

pyrolysis. In the Stage 1, the peak is observed at 105.67^{o}C with a weight loss rate of 0.04%/min. The slow rate of weight loss in this stage is attributed to the removal of bound and unbound moisture which is attached due to the surface tension and van-der Waal forces (Kumar et al., 2019b). In Stage 2, as the temperature increases the rate of % degradation is high (1.29%/min) at a temperature of 348.2^{o}C is observed. With further increase in temperature, it is observed that the rate of degradation decreases and it becomes almost constant. Lastly in Stage 3, the weight loss is almost constant (the change is as low as0.01%/min). It can be seen from Fig. 9.3 (a), that in case of PMW, there no significant peak is observed and the biomass degraded at an almost constant rate throughout the stage (Stage 2). Therefore, it can be concluded from above discussion that, the temperature range of 250 to 500^{o}C will be most suitable for bio-oil production.

9.6.4 Effect of Montmorillonite Clay

The effect of Montmorillonite clay on thermal degradation behaviour of PMW was analysed using TGA/DTG analyses and results are shown in Fig. 9.3 (a). In the first stage, approximately 8% weight loss of PMW+clay has been observed which is higher than that for PMW alone. It is also noticed from the DTG curve that, the peak temperature in the Stage 1has reduced to a lower value (75^{o}C) with a higher degradation rate of 0.69%/min compared to PMW alone. A significant increase in the rate of thermal decomposition of PMW+clay mixture has been observed in Stage 2. In this stage (250 to 450^{o}C), the weight loss was (56.67%) slightly less than that for the non-catalytic sample (PMW) while the rate of degradation (3.53%/min at 397^{o}C) is found to be higher. In Stage 3 the degradation rate is found to be slow (0.09%/min) but it was slightly higher than for PMW.

It has been observed that the presence of Montmorillonite clay has affected the pyrolysis of PMW considerably. From Fig. 9.3(a) it can be seen that, the percentage residual weight in case of catalytic pyrolysis has decreased by about 17.28% compared to 20.80% in the case of non-catalytic pyrolysis. The lower residual weight is beneficial for thermal conversion of biomass to value added products (bio-oil and gas).

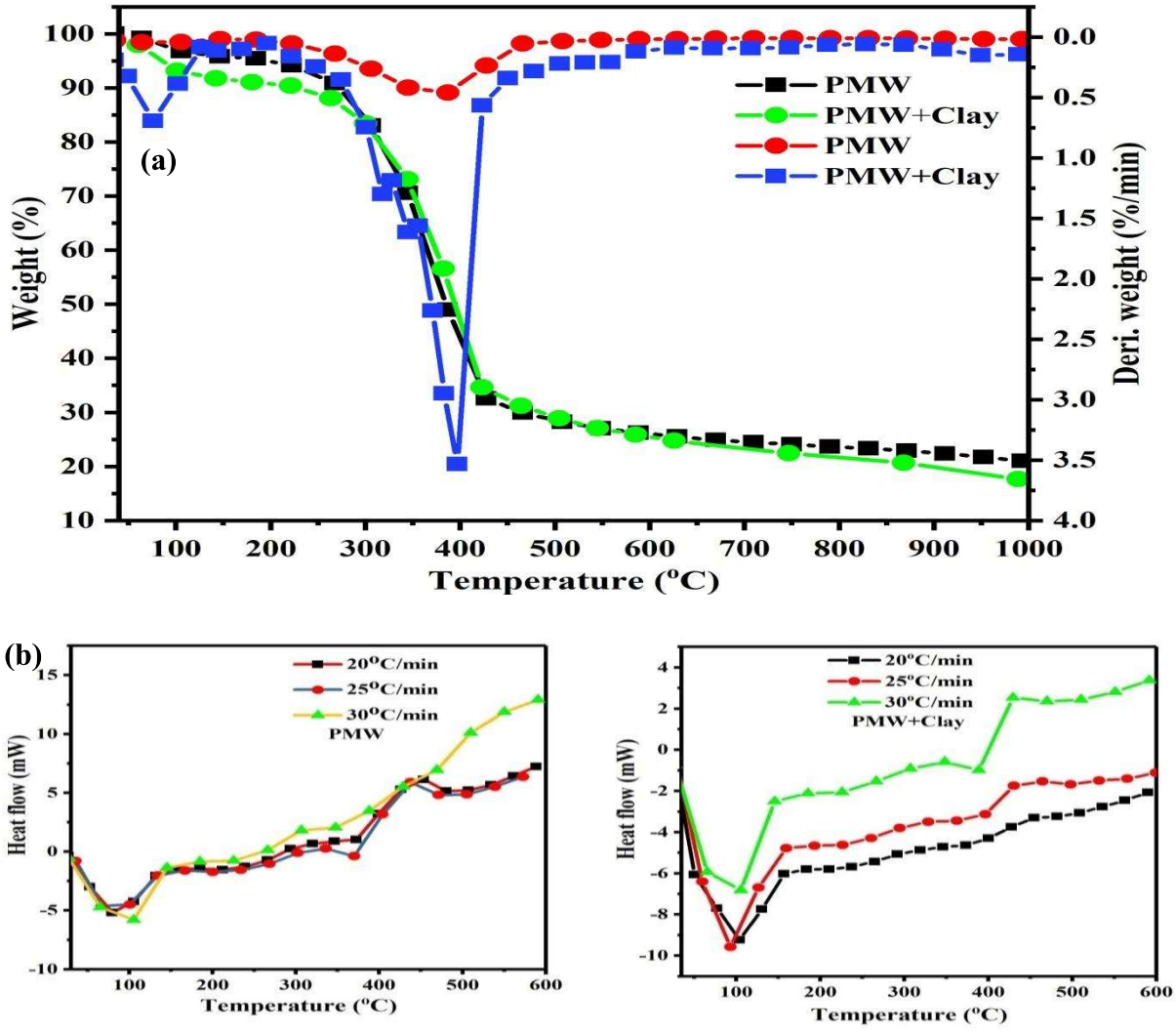

Fig. 9.3(a): TG and DTG analysis curve of PMW and PMW+Clay at 30°C/min, **(b):** Heat flow analysis during pyrolysis of paper mill waste (PMW) and PMW+Clay at 20, 25 and 30°C/min

***Deri** = Derivative weight loss (dw/dt)

9.6.5 Heat flow analysis

Differential scanning calorimetry has been used to understand the variation of the release of heat during pyrolysis with temperature and time. It indicates the endothermic or exothermic nature of the process (Leroy et al., 2006). The heat flow curves of PMW and PMW+clay samples are depicted in Fig. 9.3 (b) at the heating rates of 20, 25 and 30^{o}C/min. It is interesting to note that the Montmorillonite clay has considerable effect on the heat flow behaviour during thermal degradation of PMW. For PMW+clay and PMW samples, the DSC curves show the first peak below 150^{o}C. These peaks are attributed to the removal of moisture from the sample and indicate the endothermic nature of the process. It was observed that, as the heating rate increased from 20 to 30^{o}C/min the DSC curves shifted towards the upward direction (from endothermic to exothermic) in both the cases. Peaks observed in the temperature range of 240-500^{o}C show the thermal decomposition of main constituents (hemicellulose and cellulose) of the sample (Mishra and Mohanty, 2018).

9.6.6 Effect of heating rate

The heating rate is an important parameter that affects the rate of thermal degradation, amount of volatile matter released, and the residual weight after the completion of pyrolysis (Kumar et al., 2019b). Therefore, it affects the yield of pyrolysis products also. The TGA data at different heating rates are most useful for kinetic analysis of pyrolysis by applying ICTAC recommended iso-conversional models(Vyazovkin, 1997). The thermal degradation data for PMW and PMW+ clay mixture for three different heating rates (10, 20 and 30^{o}C) are shown as TGA (%weight versus temperature), DTG (%wt/min versus temperature) and conversion (temperature versus α) plots in Fig 9.4. The characteristic temperatures like initial temperature (T_i), final temperature (T_f), and the temperature

corresponding to the maximum degradation rate (T_P), determined using the respective TGA and DTG curves depicted in Fig. 9.4, are presented in Table 9.2.

It is seen from the Fig. 9.4 that the TGA and DTG curves have gradually shifted towards the higher temperature side with increase in the heating rate. The thermal degradation characteristics for PMW and PMW + clay samples in each stage are presented in Table 9.2. It is interesting to note that the shifting of the curves towards the higher temperature side does not affect the nature of thermal degradation behaviour (Gai et al., 2013). In case of PMW the highest thermal degradation rate was found to be 0.08%/min at 71°C at the heating rate of 20°C/min and it decreased with increase in the heating rate. On the other hand in case of PMW+clay, the highest degradation rate was 0.69%/min at 75.85°C at the heating rate of 30°C/min. It is also observed from Table 9.2 that the rate of degradation has increased in each stage and this may be attributed to the catalytic effect of the clay. In Stage 2, the rate of degradation decreases and the corresponding temperature increases with the heating rate in case of PMW. The highest rate was found to be 0.64%/min at 341°C for the heating rate of 20°C/min. In case of PMW + clay, the rate of degradation and the corresponding increase in temperatures with the heating rate is in the order of 2.58%/min (350°C) at 20°C/min < 3.08%/min (393°C) at 25°C/min < 3.57%/min (397°C) at 30°C/min. The magnitude of weight loss (%) in this stage decreases with the heating rate. In case of PMW, it has decreased from 68.25 to 59.96% while in case of PMW + clay from 56 to 55.69% for increase in heating rate from 20 to 30°C/min. In Stage 3, the rate of degradation and corresponding temperature have changed in the order: 0.23%/min (440°C) at 20°C/min > 0.19%/min (445°C) at 25°C/min >0.05%/min (450°C) at 30°C/min in case of PMW while in case of PMW + clay the order of change is as: 0.82%/min (440°C) at

20°C/min > 0.41%/min (445°C) at 25°C/min > 0.34%/min (450°C) at 30°C/min. In the last stage (Stage 3), the weight loss (%) has decreased from 16.52 to 10.14% while in case of PMW + clay from 22.72 to 14.90% for the change in the heating rate from 20 to 30°C/min. At the end of the pyrolysis (at 1000°C), the residual weight has increases from 6.8 to 20.80% in case of PMW and from 6.30 to 17.28 % in case of PMW+ clay with increase in heating rate from 20 to 30°C/min. The lower residual weight observed in case of PMW+clay clearly indicates that more volatile products and less char have formed due to the catalytic action of clay.

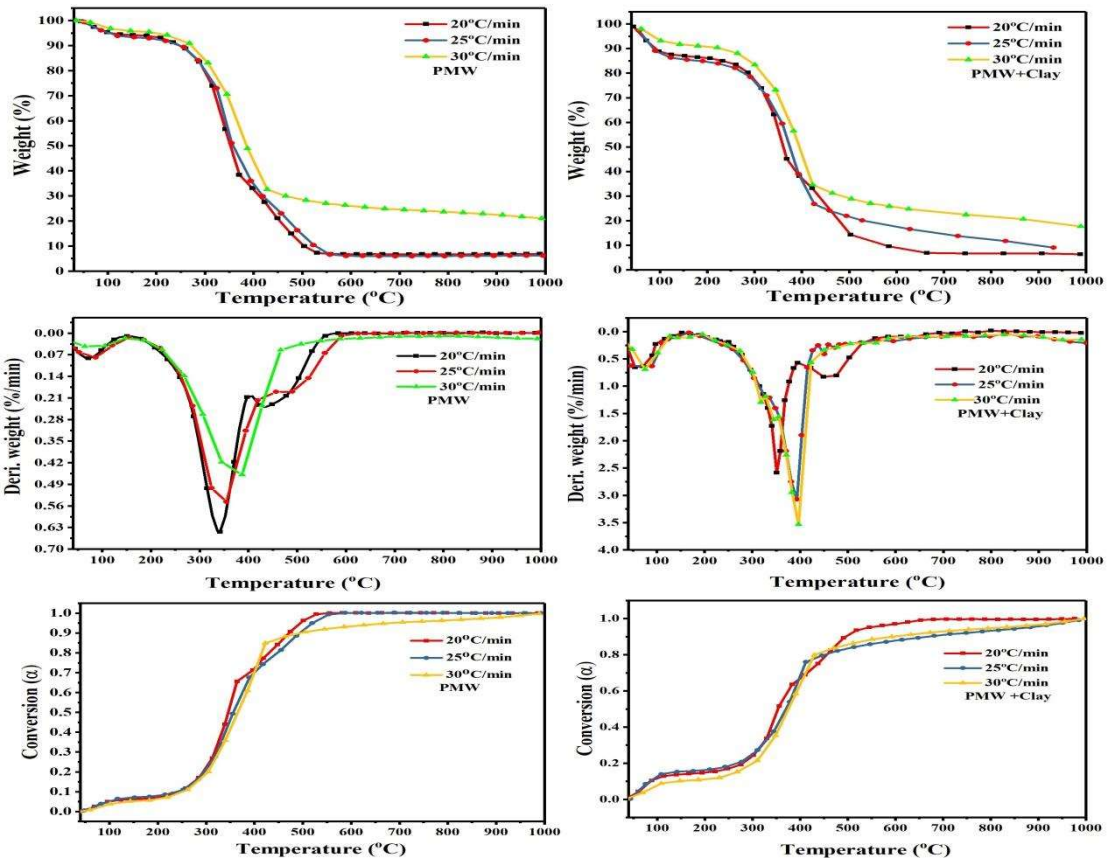

Fig.9.4 Effect of heating rate on TGA and DTG analysis pattern and conversion of PMW and PMW+Clay

9.6.7 Kinetic analysis

The kinetic analyses for the determination of activation energy and pre-exponential factor have been carried out using iso-conversional kinetic models of FWO and Vyazovkin and DAEM model. In case of FWO and DAEM models, values of activation energy and pre-exponential factor were calculated using the slopes and intercepts of the respective Arrhenius plots shown in Fig. 9.5, while in case of Vyazovkin model, these were calculated by minimizing the function given in Eq. (4.27). Due to insignificant values of the correlation coefficient (R^2) for $\alpha > 0.8$, the kinetic analysis was carried out in the conversion (α) range of 0.1 to 0.8.The values of activation energy (E_α) and pre-exponential factor (A) at each conversion and their average values for all three models are reported in Table 9.3. The variation of activation energy with conversion using FWO, DAEM and Vyzovkin models is also depicted in Fig. 9.6. The values of R^2 (> 0.99) at each conversion using FWO and DAEM model are also presented in Table 9.3. For the conversion of 0.1 to 0.2, the value of E_α has increased from 176.22 to 192.57kJ/mol for PMW and from 166.98 to 192.09kJ/mol for PMW+clay that are marginally lower. The increment may be attributed to the starting of removal of hemicellulose and cellulose fraction (Mishra and Bhaskar, 2014). In case of FWO model, from Fig. 9.6 and Table 9.3 it can be seen that the values of activation energy decrease from 171.84 to 93.56kJ/mol and 166.54 to 67.26kJ/mol as conversion increases from 0.3 to 0.5 for PMW and PMW+clay respectively.

The reason for this is that the hot vapor and light volatile matter released from hemicellulose and cellulose provided heat to the sample. Thus, this led to the need of less activation energy for degradation up to $\alpha = 0.5$.Further, as conversion increases the activation energy increases from 109.21 to 276.62kJ/mol and 123.99 to 268.92kJ/mol up to $\alpha = 0.7$ and after that a slight decrease in activation energy at $\alpha = 0.8$ conversions. Almost similar trend of variation have been observed

regarding activation energy variation with conversion using DAEM and Vyazovkin model (Table 9.3).

The average activation energy (E_α) in case of non-catalytic PMW pyrolysis was found to be 174.30, 286.32 and 184.32kJ/mol using FWO, DAEM and Vyzovkin model respectively while in case of PMW+clay the corresponding values were found to be 166.19, 257.20 and 173.25kJ/mol respectively.

The values of pre-exponential factor (A) are presented in Table 9.3. In general it indicates that the degree of collision of reactant of pyrolysis system per unit time (Fong et al., 2019). For non-catalytic sample PMW the values of A from $\alpha = 0.1$ to 0.8 are 5.43E+12 to 2.05E+21, 6.24E+22 to 9.69E+21 and 4.61E+13 to 3.98E+23min^{-1} using FWO, DAEM and Vyzovkin models respectively. For PMW + clay sample, the corresponding A values are 8.64E+11 to 1.99E+20, 4.02E+20 to 2.50E+22 and 4.26E+12 to 9.52E+21min^{-1} respectively.

The average values of A for PMW was found to be 5.36E+20, 5.71E+23 and 7.74E+22min^{-1} using FWO, DAEM and Vyzovkin models respectively while in case of PMW + clay the corresponding average values of A were found to be 8.62E+19, 2.50E+22 and 5.90E+21min^{-1} respectively.

The consistently lower values of A and E_a for PMW+ clay mixture compared to PMW alone indicate that Montmorillonite plays a catalytic role in the pyrolysis of paper mill waste biomass.

Table 9.3: Kinetic and Thermodynamics of PMW and PMW+Clay

	PMW						PMW+Clay					
Conversion (α)	**E_α(kJ/ mol)**	**R^2**	**A(s^{-1})**	**ΔH(kJ/ mol)**	**ΔG(kJ/ mol)**	**ΔS(kJ/ mol.K)**	**E_α(kJ/ mol)**	**R^2**	**A(s^{-1})**	**ΔH(kJ /mol)**	**ΔG(kJ /mol)**	**ΔS(kJ/ mol.K)**
FWO												
0.1	176.22	0.9968	5.43E+12	171.60	180.35	-14.04	166.98	0.9925	8.64E+11	162.27	180.63	-29.46
0.2	192.57	0.9923	1.39E+14	187.72	179.89	12.58	192.09	0.9945	1.27E+14	187.13	179.90	11.60
0.3	171.84	0.9991	2.27E+12	166.84	180.48	-21.89	166.54	0.9990	7.91E+11	161.43	180.64	-30.83
0.4	98.18	1.0000	8.65E+05	93.06	183.38	-144.97	79.37	0.9949	1.85E+04	74.17	184.48	-177.07
0.5	93.56	0.9976	3.37E+05	88.37	183.63	-152.90	67.26	0.9954	1.51E+03	61.97	185.33	-198.02
0.6	109.21	0.9991	8.09E+05	103.90	182.83	-126.69	123.99	0.9989	1.59E+08	118.54	182.17	-102.12
0.7	276.62	0.9998	2.23E+21	271.09	178.01	149.40	268.92	0.9998	4.90E+20	263.29	178.16	136.64
0.8	276.20	0.9923	2.05E+21	270.45	178.02	148.41	264.34	0.9988	1.99E+20	258.38	178.25	128.64
Avg.	174.30		5.36E+20	169.13	180.82	-18.76	166.19		8.62E+19	160.89	181.20	-32.58
DAEM												
0.1	293.57	0.9947	6.24E+22	288.98	177.71	178.60	267.92	0.9941	4.02E+20	263.25	178.18	136.55
0.2	314.99	0.9984	4.19E+24	310.17	177.34	213.21	298.98	0.9999	1.80E+23	294.06	177.61	186.91
0.3	296.25	0.9932	1.06E+23	291.27	177.66	182.36	286.95	0.9930	1.70E+22	281.86	177.82	166.99
0.4	268.99	0.9914	4.97E+20	263.87	178.16	137.58	218.92	0.9995	2.56E+16	213.72	179.22	55.36

0.5	254.07	0.9969	2.64E+19	248.88	178.45	113.04	182.99	0.9986	2.08E+13	177.70	180.15	-3.94
0.6	279.26	0.9924	3.75E+21	273.96	177.96	154.08	274.28	0.9991	1.41E+21	268.84	178.06	145.73
0.7	299.32	0.9971	1.93E+23	293.85	177.60	186.59	261.08	0.9987	1.05E+20	255.46	178.31	123.83
0.8	284.09	0.9955	9.69E+21	278.37	177.88	161.30	266.44	0.9902	3.01E+20	260.51	178.21	132.11
Avg.	286.32		5.71E+23	281.17	177.85	165.85	257.20		2.50E+22	251.92	178.45	117.94
Vyazovkin												
0.1	187.00		4.61E+13	182.38	180.04	3.76	175.00		4.26E+12	170.29	180.38	-16.20
0.2	209.00		3.60E+15	204.15	179.45	39.63	203.00		1.10E+15	198.04	179.62	29.57
0.3	181.00		1.40E+13	176.00	180.21	-6.76	175.00		4.26E+12	169.89	180.38	-16.84
0.4	97.00		6.81E+05	91.88	183.44	-146.97	74.00		6.12E+03	68.79	184.84	-186.27
0.5	91.00		2.00E+05	85.81	183.77	-157.24	59.00		2.69E+02	53.71	186.02	-212.37
0.6	110.00		9.50E+05	104.69	182.79	-125.36	125.00		1.95E+03	119.55	182.13	-100.45
0.7	300.00		2.20E+23	294.47	177.59	187.60	291.00		3.77E+22	285.37	177.75	172.74
0.8	303.00		3.98E+23	297.28	177.54	192.19	284.00		9.52E+21	278.05	177.88	160.79
Avg.	184.75		7.74E+22	179.58	180.61	-1.64	173.25		5.90E+21	167.96	181.13	-21.13

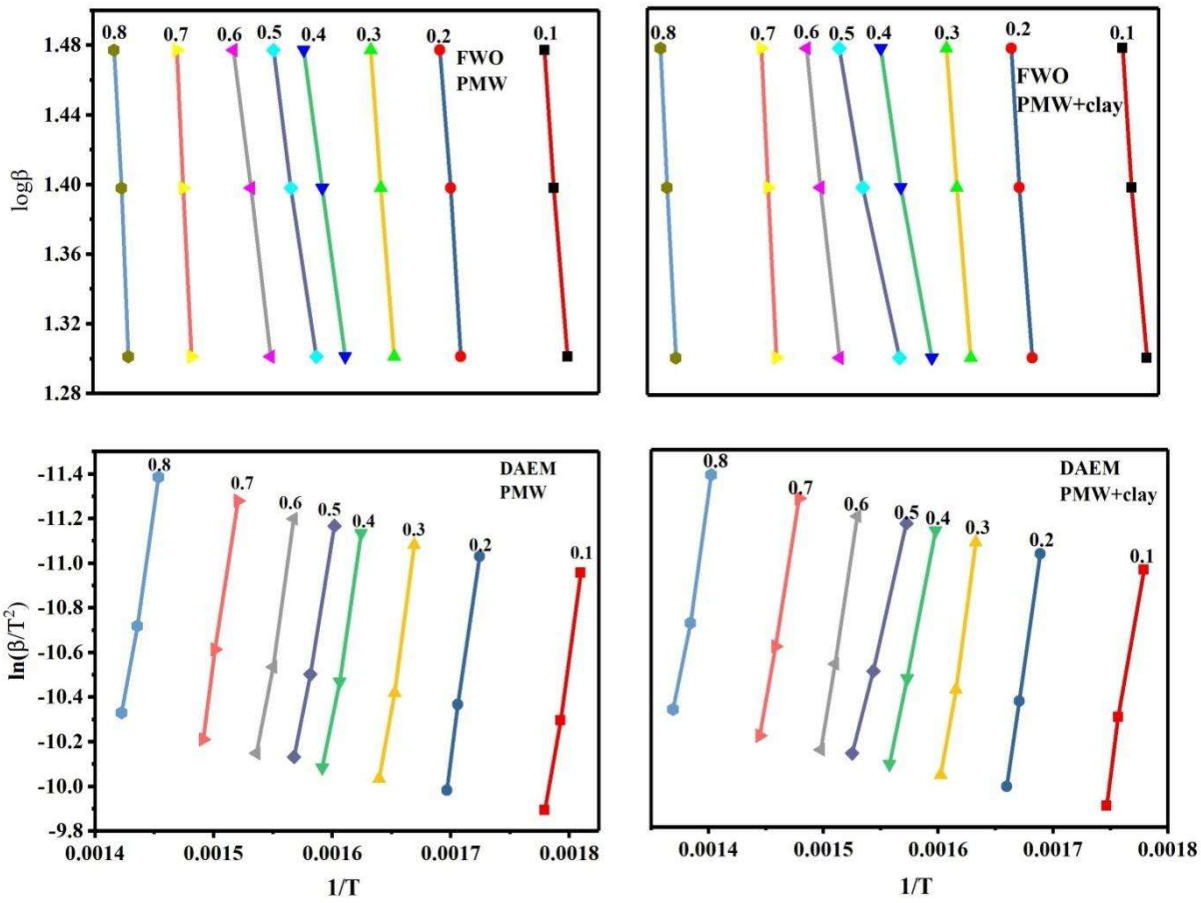

Fig. 9.5 Arrhenius plots of PMW and PMW+Clay using FWO and DAEM

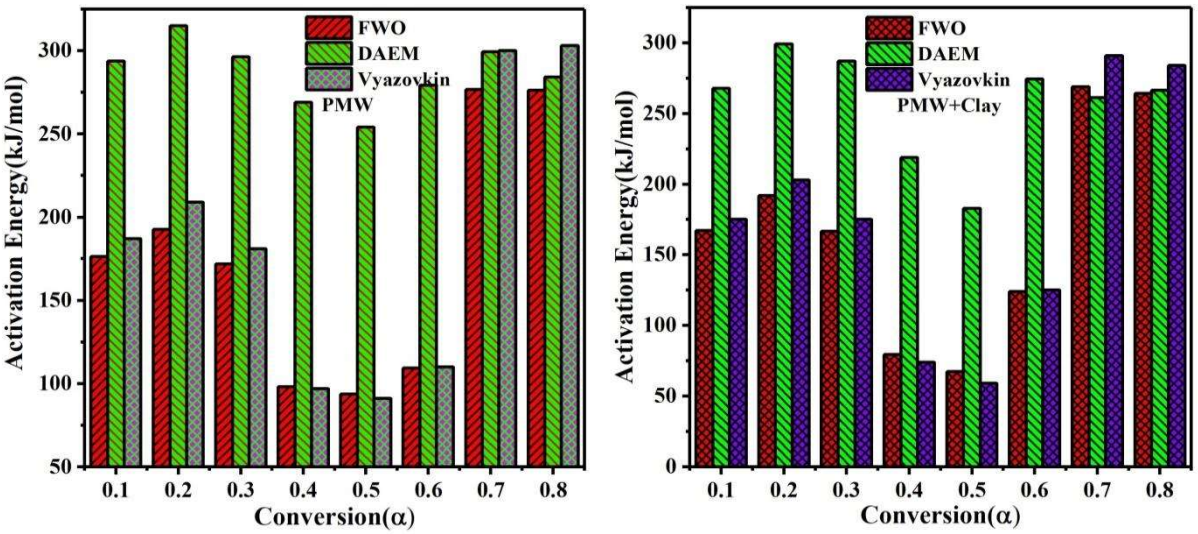

Fig.9.6 Variation of activation energy with conversion of PMW and PMW+Clay using FWO, DAEM and Vyazovkin kinetic models

9.6.8 Thermodynamic parameters

The thermodynamic parameters (ΔH, ΔG, ΔS) were calculated for conversion values of 0.1 to 0.8 using the values of energy of activation calculated from FWO, DAEM and Vyzovkin models. Values of all three parameters at each conversion level together with their average values are listed in Table 9.3 and are graphically depicted in Fig.9.7.

It is seen from Table 9.3 that difference between the energy of activation and that consumed during the pyrolysis is on an average less than 5kJ/mol and this shows that there is no potential barrier between the paper mill waste and its corresponding activated complex. In case of PMW values of ΔH obtained using FWO, DAEM, and Vyzovkin models vary in the range of 88.37 to 270.45, 248.88 to 310.17, and 85.81 to 297.28kJ/mol, respectively while for PMW+clay it varies from 61.97 to 263.29, 177.70 to 294.06 and 53.71 to 285.37kJ/mol respectively.

For PMW, the ΔG values for FWO, DAEM, and Vyzovkin models were found to be 178.01 to 183.63, 177.34 to 178.45, and 177.54 to 183.44kJ/mol, respectively while for PMW + clay ΔG were found to vary as 178.16 to 185.33, 177.62 to 180.15 and 177.75 to 186.02kJ/mol respectively.

The calculated values of ΔS at each conversion level are presented in Table 9.3. The ΔS values are both negative and positive. Negative values of ΔS indicate that the randomness of product formed from degradation of bond of reactant was lower than the initial reactant (Mehmood et al., 2017). Both negative and positive values are attributed to the complexity of the biomass pyrolysis process (Gupta and Mondal, 2019).

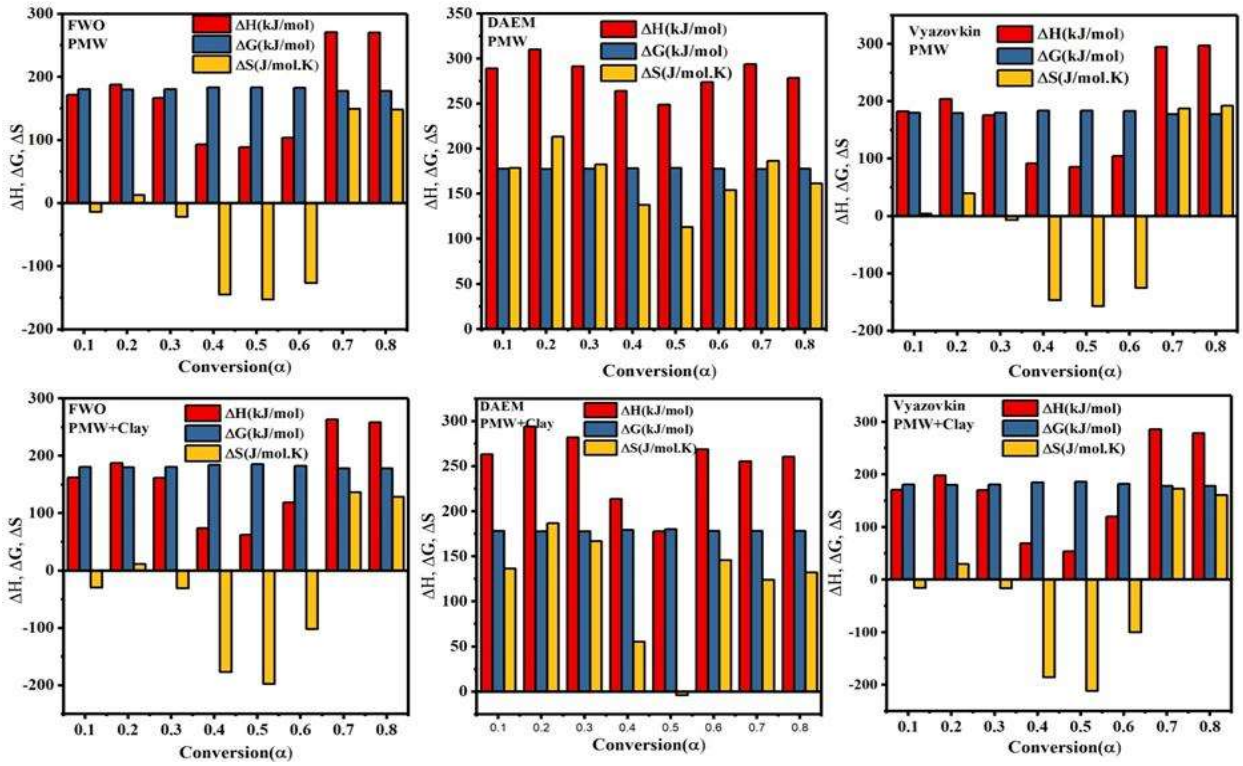

Fig 9.7: Variation of thermodynamic parameters using FWO, DAEM and Vyazovkin model

9.6.9 The Reaction Mechanism of Pyrolysis

Figure 9.8 depicts the plots of theoretical Z-master values calculated using the algebraic equations listed in Table 4.2 and Eq. 4.52 versus conversion. The experimental Z-master values calculated using Eq. 4.52 is also plotted on the same graph for comparison.

It is clear from Fig. 9.8 that no single reaction mechanism is followed by the experimental data over the entire conversion range. The experimental curve for PMW follows the theoretical curves F_1 (nucleation with one nucleus on the individual particle), D_1 (one-dimensional diffusion), D_2 (two-dimensional diffusion-Valensi model)), D_3 (three-dimensional diffusion-Jander model), and D_4 (three-dimensional diffusion- Ginstlinge-Brounshtein model)) quite closely up to the conversion of 0.2. For $\alpha = 0.2$ to 0.3 no exact

mechanism is discernible probably due to the simultaneous dissociation of large molecules comprising the biomass in to smaller molecules. For the conversion values of 0.3 to 0.5 experimental curve follows the theoretical curves for equations A_1 (nucleation and growth (Avrami-Eq.1), A_3 (nucleation and growth- Avrami Eq.3)), D_3 and P_4 (power law). At higher conversion rates (a > 0.5), the experimental data follows the theoretical curves for equations D_4 and F_1very closely. In the presence of catalyst, the experimental curve for α< 0.1 overlaps the theoretical curve for equation R_3 (the phase boundary-controlled reaction-contracting volume model). Like PMW, in this case also for conversion from 0.2 to 0.3, no mechanism is clearly discernible. In the conversion range of 0.3 to 0.5, the experimental data coincide with theoretical curves for equations P_4, A_1, D_1, D_2 and D_4. For the conversion range 0.5 to 0.8 the experimental curve is very close to the curve for equation R_2 (phase boundary-controlled reaction with contracting area).

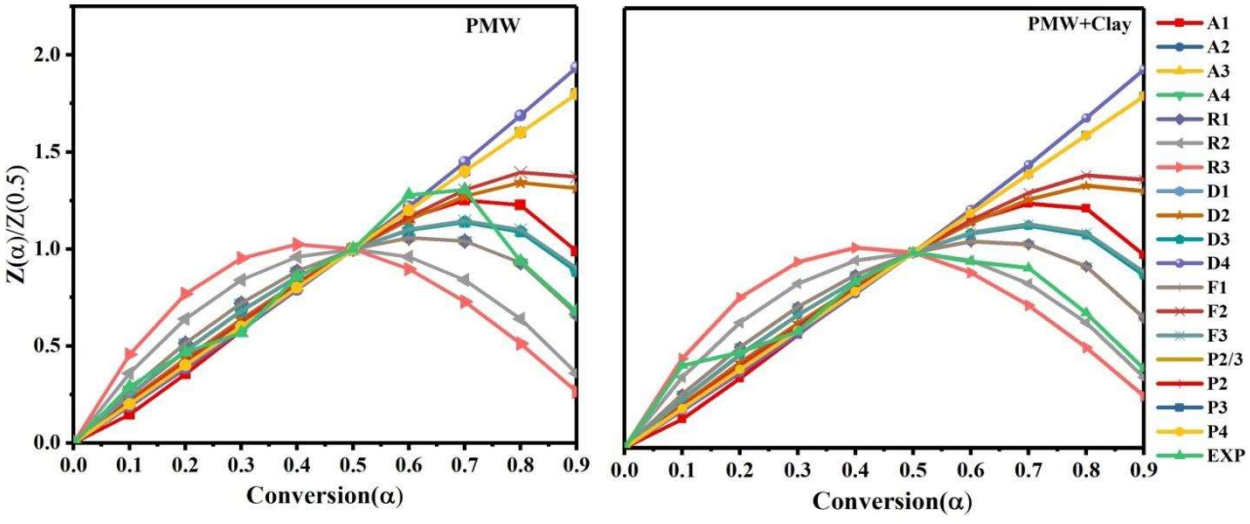

Fig. 9.8 Reaction mechanism of PMW and PMW+Clay

9.7 Conclusion

The paper mill waste is a suitable industrial waste biomass for use as fuel. Its pyrolysis in presence of a solid catalytic material like Montmorillonite clay has a positive effect on its thermal degradation behaviour and related kinetic and thermodynamic parameters. Presence of catalyst resulted in reduced residual weight at each heating rate. The rate of thermal degradation increased significantly in presence of clay. The activation energy also decreased using all the models. The FWO model gave the lowest activation energy for both catalytic (PMW +clay) and non-catalytic (PMW) pyrolysis. Remarkable changes were observed in experimental curve of Z-master plot depicting the reaction mechanism.